

## **General Disclaimer**

### **One or more of the Following Statements may affect this Document**

- This document has been reproduced from the best copy furnished by the organizational source. It is being released in the interest of making available as much information as possible.
- This document may contain data, which exceeds the sheet parameters. It was furnished in this condition by the organizational source and is the best copy available.
- This document may contain tone-on-tone or color graphs, charts and/or pictures, which have been reproduced in black and white.
- This document is paginated as submitted by the original source.
- Portions of this document are not fully legible due to the historical nature of some of the material. However, it is the best reproduction available from the original submission.

**NASA TECHNICAL  
MEMORANDUM**

**NASA TM X-62, 440**

**NASA TM X-62, 440**

(NASA-TM-X-62440) A FILM-RUPTURE MODEL OF  
HYDROGEN-INDUCED, SLOW CRACK GROWTH IN  
ALPHA-BETA TITANIUM (NASA) 24 p HC \$3.25  
CSCL 11F

N75-24903

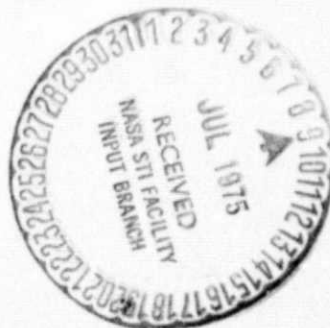
Unclas  
G3/26 26397

**A FILM-RUPTURE MODEL OF HYDROGEN-INDUCED, SLOW CRACK GROWTH  
IN ALPHA-BETA TITANIUM**

**Howard G. Nelson**

**Ames Research Center  
Moffett Field, California 94035**

**June 1975**



1. Report No. <b>NASA TM X-62, 440</b>	2. Government Accession No.	3. Recipient's Catalog No.	
4. Title and Subtitle <b>A FILM-RUPTURE MODEL OF HYDROGEN-INDUCED, SLOW CRACK GROWTH IN ALPHA-BETA TITANIUM</b>		5. Report Date	
		6. Performing Organization Code	
7. Author(s) <b>Howard G. Nelson</b>		8. Performing Organization Report No. <b>A-6088</b>	
		10. Work Unit No. <b>505-01-21-02-00-21</b>	
9. Performing Organization Name and Address <b>NASA-Ames Research Center Moffett Field, California 94035</b>		11. Contract or Grant No.	
		13. Type of Report and Period Covered <b>Technical Memorandum</b>	
12. Sponsoring Agency Name and Address <b>National Aeronautics and Space Administration Washington, D.C. 20546</b>		14. Sponsoring Agency Code	
15. Supplementary Notes			
16. Abstract <p>The appearance of the terrace-like fracture morphology of gaseous hydrogen-induced crack growth in acicular alpha-beta titanium alloys is discussed as a function of specimen configuration, magnitude of applied stress intensity, test temperature, and hydrogen pressure. Although the overall appearance of the terrace structure remained essentially unchanged, a distinguishable variation is found in the size of the individual terrace steps, and step size is found to be inversely dependent upon the rate of hydrogen-induced slow crack growth. Additionally, this inverse relationship is independent of all the variables investigated. These observations are quantitatively discussed in terms of the formation and growth of a thin hydride film along the alpha-beta boundaries and a qualitative model for hydrogen-induced slow crack growth is presented, based on the film-rupture model of stress corrosion cracking.</p>			
17. Key Words (Suggested by Author(s)) <b>Fracture morphology Alpha-beta titanium alloys Hydrogen-induced crack growth</b>		18. Distribution Statement  <b>Unclassified — Unlimited</b>  <b>STAR Category — 26</b>	
19. Security Classif. (of this report) <b>Unclassified</b>	20. Security Classif. (of this page) <b>Unclassified</b>	21. No. of Pages <b>22</b>	22. Price* <b>\$3.25</b>

**A FILM-RUPTURE MODEL OF HYDROGEN-INDUCED, SLOW CRACK GROWTH  
IN ALPHA-BETA TITANIUM**

**Howard G. Nelson**

A unique fracture morphology is associated with gaseous hydrogen-induced crack growth in the alpha-beta titanium alloys of 6Al-4V,<sup>1</sup> 5Al-2.5Sn,<sup>2</sup> and 8Al-1Mo-1V<sup>3</sup> when these alloys have a microstructure of acicular alpha-phase platelets in a continuous beta-phase matrix. Fig. 1 is a scanning electron micrograph (SEM) of a typical fracture surface that illustrates the common features of this unique morphology. As seen from this figure, the fracture surface is made up of a terrace-like structure consisting of groups of parallel, evenly spaced facets bowed in the direction of what appears to be local crack growth (indicated by the arrows). It has been suggested<sup>1</sup> that this terrace-like structure is associated with intergranular separation along alpha-beta boundaries due to the formation and brittle rupture of thin hydride films formed within the alpha-phase platelets at the alpha-beta boundaries. Pittinato and Hanna<sup>4</sup> have since shown that hydrogen is preferentially absorbed from the environment into the beta-phase and that titanium hydride can in fact precipitate out in the alpha-phase at the alpha-beta boundaries. Additionally, Meyn<sup>3</sup> observed that the terrace fracture facets nearly always occur on planes close to the  $\{1010\}_\alpha$  planes — the normal habit planes for titanium hydride precipitation in alpha-phase titanium and the planes generally thought to be parallel to the long axis of the alpha-phase platelets in an acicular microstructure.<sup>5,6</sup>

From previous studies on gaseous hydrogen-induced crack growth in titanium,<sup>1,2,7</sup> it has been postulated that the continuous beta-phase network present in an acicular alpha-beta titanium structure acts as a "short-circuit" transport path for hydrogen and permits hydrogen to penetrate more rapidly into the titanium lattice than if the beta-phase were discontinuous or if only the alpha-phase were present. Near room temperature, hydrogen transport in beta-phase titanium is several orders of magnitude more rapid than in alpha-phase titanium.<sup>8</sup> Once hydrogen exists in the beta-phase ahead of the crack tip, embrittlement occurs in much the same manner as postulated by Craighead et al.<sup>9</sup> for hydrogen-charged alpha-beta titanium alloys. These authors put forth the original idea that hydrogen within the beta-phase can segregate at the alpha-beta boundaries and result in intergranular separation.

The purpose of this paper is to present a semi-quantitative interpretation of the terrace-like fracture morphology observed in the gaseous hydrogen-induced cracking of acicular alpha-beta titanium. Specifically, an attempt is made to establish the influence of stress intensity, temperature, and hydrogen pressure on the appearance of the terrace-like fracture morphology, and to relate these observations to corresponding variations in crack growth rate. Finally, an attempt is made to quantitatively explain the observations of crack growth kinetics and fracture morphology by a film-rupture model of stress corrosion cracking applied to the formation and rupture of a thin hydride film.

## EXPERIMENTAL PROCEDURE

The material used for this investigation was commercially produced Ti-6Al-4V alloy in the form of 0.32-cm and 1.27-cm thick plates. The material was machined into specimens and solution-treated at 1040°C for 40 min, stabilized at 700°C for 1 hr and at 590°C for 1 hr in vacuum, and then air-cooled to produce a microstructure of acicular alpha-phase platelets in a continuous beta-phase matrix.<sup>1</sup>

Two types of specimens were used; the wedge-opening-loaded, double-cantilever-beam (DCB) specimen described by Mostovoy et al.<sup>10</sup> and the double torsion (DT) specimen discussed by Williams and Evans.<sup>11</sup> The former specimen type was used with the 1.27-cm thick plate and the latter with the 0.32-cm thick plate stock. Both specimen types were tested under conditions of fixed displacement and thus the stress intensity decreased as the cracks grew, permitting a high degree of control of crack growth. The specimens were precracked by fatigue in gaseous hydrogen prior to testing and crack growth rates were continuously monitored by measurement of compliance change.<sup>2,11</sup>

All tests were conducted in a stainless-steel, metal-sealed, test chamber that was evacuated to at least  $10^{-1}$  N m<sup>-2</sup> prior to backfilling with hydrogen to the desired test pressures. Hydrogen gas was laboratory-grade that initially contained less than 100 ppm active impurity gases (O<sub>2</sub>, H<sub>2</sub>O, N<sub>2</sub>); the gas was additionally dried by passing it slowly through liquid-nitrogen-cooled coils. Specimen and gas temperatures were varied below room temperature by use of a liquid or cold-gaseous nitrogen-chilled baffle surrounding the specimen within the test chamber. Specimen temperature was monitored by thermocouples spot-welded to the specimen surface near the path of the propagating crack.

The morphology of the fracture surfaces was studied using a scanning electron microscope. Comparisons between fracture morphology and crack growth rate were made through a correlation of crack length using the applicable compliance equations.<sup>10,11</sup> The width,  $X$ , of the individual terrace steps at any location on the fracture surface was determined by using an intercept method and always involved averaging over at least 20 terrace steps.

## EXPERIMENTAL RESULTS

In an effort to identify variations in terrace morphology with stress intensity and/or crack growth rate, a DT specimen was tested at 24°C in gaseous hydrogen at 90.6 kN m<sup>-2</sup> and the fracture

surface studied in detail as a function of crack length. Because specimen displacement was held constant in this test, stress intensity decreased from  $62 \text{ MN m}^{-3/2}$  to  $20 \text{ MN m}^{-3/2}$  as the crack length increased. Although the appearance of the terrace structure was found to remain essentially unchanged over the entire length of hydrogen-induced crack growth, a variation was found in the size of the individual terrace steps depending on location along the crack. This variation in step width,  $X$ , as a function of crack length,  $a$ , is shown in Fig. 2; as can be seen,  $X$  increases as  $a$  increases. Also shown in Fig. 2 is the logarithm of the rate of hydrogen-induced crack growth,  $V$ , observed in this specimen as a function of  $a$ . As shown, crack growth rate decreased with increasing crack length. These dependences of  $X$  and  $\log V$  on crack length suggest that an inverse relationship may possibly exist between these two parameters. (As we will see, this inverse relationship is found in all experiments of this study.) Additionally, in view of the fact that stress intensity varies as a simple inverse function of crack length in a DT specimen,<sup>11</sup> this simple dependence of  $K$  on crack length suggests that  $X$  is not a direct function of  $K$ .

A similar study was conducted using a different specimen configuration (DCB specimens) over a greater range of stress intensities and at two temperatures:  $24^\circ\text{C}$  and  $-10^\circ\text{C}$ . Figs. 3 and 4 are plots of logarithms  $V$  and  $X$ , respectively, as functions of applied stress intensity. As seen in Fig. 3, crack growth at both temperatures exhibits the usual complex dependence on stress intensity —  $V$  increasing rapidly with  $K$  at low values of  $K$  (Stage I), less rapidly at intermediate  $K$  values (Stage II), and again rapidly as  $K$  approaches the critical stress intensity (Stage III). Additionally, a decrease in temperature from  $24^\circ\text{C}$  to  $-10^\circ\text{C}$  is seen to decrease the crack growth rate for any given stress intensity. Step width was also found to exhibit a complex dependence on applied stress intensity as shown in Fig. 4. As stress intensity increases,  $X$  was observed to decrease rapidly in the region of Stage I, to level off in Stage II, and to decrease rapidly in Stage III. As with the previous observations, these results again indicate that  $X$  is inversely related to some function of  $V$ . As would be expected, a decrease in temperature is seen to result in a decrease in crack growth rate and, thus, an increased step width for a given value of stress intensity.

Using DT type specimens, the variation in  $X$  as a function of hydrogen pressure was studied as a constant applied stress intensity in the region of Stage II. Table I is a tabulation of these results. As can be seen,  $V$  decreased with decreasing hydrogen pressure in a manner similar to that previously reported,<sup>2,7</sup> whereas  $X$  increased — again, suggesting some type of inverse relationship.

The variation in  $X$  as a function of  $V$ , observed in all experiments of this study, is summarized in Fig. 5. This figure is a plot of logarithm  $V$  versus logarithm  $X$  and includes all data of this

investigation: the DT specimen tested at 24°C in hydrogen at 90.6 kN m<sup>-2</sup> (Fig. 2), DCB specimens tested at 24°C and -10°C at 90.6 kN m<sup>-2</sup> (Figs. 3 and 4), and DT specimens tested at various hydrogen pressures at 24°C at a constant stress intensity in Stage II (Table I). Although a fair amount of scatter exists in the data, step width is found to increase as crack growth rate is decreased. As seen in Fig. 5, the data of the individual experiments appear to be randomly distributed throughout the band of scatter, thus suggesting that this relationship is independent of the variables of specimen configuration, magnitude of applied stress intensity, hydrogen pressure, and test temperature within the resolution of this study.

In an effort to describe mathematically the relationship between  $X$  and  $V$ , the data of Fig. 5 were analyzed using least-mean-squares analysis. The best-fit curve through these data appears to be either a power or an exponential relationship as shown by the dashed and solid lines, respectively. Both curves appear to fit the data equally well and are described by the following two equations:

$$V = 1.0 \times 10^{-22} X^{-4.0} \quad (1)$$

and

$$V = 1.25 \times 10^{-3} \exp(-8 \times 10^5 X) \quad (2)$$

A great many fracture facets were studied at high magnification in detail in an effort to establish whether plastic deformation of the titanium matrix is associated with individual terrace steps. In nearly all cases some plastic deformation at the forward edge of the terrace step could be identified. Fig. 6 is an example of terrace steps exhibiting rather gross evidence of plastic deformation and is typical of observations made on many fracture facets. In this figure, mating fracture surfaces are shown. Considerable plastic deformation is seen to be associated with the forward edge of the terrace steps. The fracture surface on the left is seen to contain fingers of metal which appear to have been pulled in a ductile manner from the mating fracture surface shown on the right.

## DISCUSSION

In acicular titanium, an inverse relationship has been found between the width of terrace steps observed on the fracture surface and the rate of hydrogen-induced slow crack growth [Eq. (1) or (2)]. The additional observations that this relationship seems unaffected by the variables of specimen configuration, hydrogen pressure, test temperature, and the magnitude of applied stress intensity suggest that the terrace structure is not an artifact of the crack growth process but, instead,



that crack growth occurs as the result of some failure process directly related to the terrace structure. These observations appear consistent with the idea that hydrogen-induced slow crack growth occurs by the discontinuous formation and rupture of thin titanium hydride films formed in alpha-titanium at the alpha-beta boundaries.<sup>1</sup> The terrace facets are then the result of the discontinuous brittle fracture of titanium hydride. If this were the case, the rate of slow crack growth,  $V$ , should be related to the rate of hydride film formation along the alpha-beta boundaries ahead of the crack tip (i.e.,  $dX/dt$ );

$$V = k_1 dX/dt \quad (3)$$

(To simplify this discussion the constants  $k_1, k_2, k_3, \dots k_9$ , will be introduced without explanation, since their meanings are obvious.)

Eqs. (1) and (2), then, can be rewritten, in terms of the rate of film growth along the alpha-beta boundaries, respectively, as

$$\frac{dX}{dt} = k_2 X^{-4.0} \quad (4)$$

and

$$\frac{dX}{dt} = k_3 \exp(-k_4 X) \quad (5)$$

Now, integrating these two expressions we obtain the following expressions, either of which could describe the time dependence of film growth;

$$X^5 = k_5 t + k_6 \quad (6)$$

and

$$X = k_7 \ln(k_8 t + k_9) \quad (7)$$

The former expression is a fifth-order growth law whereas the latter is a direct logarithmic law.

A fifth-order growth law is not observed in normal film forming phenomena such as in the oxidation of metals. Most such processes obey a power-law with an exponent of two (parabolic growth law) or under conditions where the film becomes protective, a cubic law is often observed. The greater the exponent, the more protective is the film, and the more completely does film growth inhibit itself. A fifth-order growth law would indicate a very stifling process and under such conditions, it becomes difficult to distinguish the exact form of the growth law, that is, a power-law, a logarithmic law, or an inverse logarithmic law. While either Eq. (6) or Eq. (7) fits the data well (Fig. 5), Eq. (6) is unreasonable and thus, a logarithmic growth law will be assumed.

A number of theories have been developed to explain logarithmic growth of an oxide film on a metal surface. Mott<sup>12</sup> and others have invoked electron tunneling through the film and Lansberg<sup>13</sup> and others have assumed chemisorption as the rate controlling processes. Evans<sup>14</sup> and Davies et al.<sup>15</sup> have proposed a model in which transport is assumed to occur preferentially along paths of low diffusion resistance — these paths eventually becoming deactivated or blocked, in time, by the reaction product. This latter model, of course, is similar to that postulated for hydrogen transport in acicular titanium<sup>1</sup> where the beta-phase acts as a path of low resistance. As the hydrogen reacts with the alpha-phase titanium at the alpha-beta boundaries to form titanium hydride, hydrogen transport in the beta-phase becomes blocked in time by the growth of the more voluminous titanium hydride.

In the remainder of this discussion we first explore the applicability of the ideas of Davies et al.<sup>15</sup> to the formation of a hydride film along the alpha-beta boundaries in acicular titanium. Next, we consider a model for crack growth based on progressive formation and rupture of the hydride film. Finally, we attempt to test this film-rupture model with the observations of this study, including the observed influences of stress intensity, hydrogen pressure, and test temperature on crack growth rate and terrace step width.

### **A Model for Hydride Film Growth along Alpha-Beta Boundaries**

It has been suggested by Davies et al.<sup>15</sup> that the logarithmic, low-temperature oxidation of an iron surface occurs by the relatively rapid movement of oxygen through discrete pores in the oxide film. As oxidation continues, these pores, in time, become blocked. An analogy may be made between this form of oxidation and the growth of a hydride film into an acicular titanium microstructure. Here, a thin continuous beta matrix (approximately 10 volume pc) separates the alpha-phase. Much like the pores in an iron oxide, hydrogen transport in beta titanium is relatively rapid. Initially, hydrogen preferentially enters the beta lattice at the crack tip and moves inward under a concentration gradient. As the hydrogen concentration along the thin beta-phase reaches a value of about 650 ppm,<sup>4</sup> hydrogen in the surface layer of the alpha-phase at the alpha-beta boundary, in equilibrium with hydrogen in the beta-phase, begins to transform to titanium hydride. The formation of titanium hydride, having a 17.2 pc greater volume than the alpha titanium it replaces,<sup>4</sup> results in a compression of the surrounding titanium lattice. The magnitude of this compression will be dependent on the thickness of the hydride film and thus, on the amount of hydrogen taken up by the beta-phase at any point in time. Because hydrogen dissolved in beta expands the lattice,<sup>4,16</sup>

the compressive strain in the beta lattice, as the result of continued growth of the titanium hydride film in the alpha phase, will make hydrogen entry and migration within the beta lattice more and more difficult, slowing hydrogen ingress, reducing the rate of hydride film advancement, and eventually blocking hydrogen movement through this path of once low resistance. Based on analogy with the model of Davies, a logarithmic expression for hydride film growth would be expected.

### **A Film-Rupture Model for Hydrogen-Induced Crack Growth**

A film-rupture model of stress corrosion cracking was first outlined by Forty<sup>17</sup> in 1959. Since that time it has undergone a number of modifications,<sup>18,19</sup> one of the more recent of which is that of Pugh,<sup>20</sup> who considered the potential influence of preferential film growth along grain boundaries. Using this work as a base, a similar model can be applied to hydrogen-induced cracking of acicular titanium where preferential hydride film growth occurs along the alpha-beta boundaries.

Initially, in acicular titanium, hydrogen enters the beta matrix and moves about relatively freely under the influence of a concentration gradient. As discussed previously, at some critical hydrogen concentration within the beta lattice, titanium hydride begins to form in the alpha-phase at the alpha-beta boundaries. This critical hydrogen concentration will first be achieved at or very near the gas-metal interface where the hydrogen concentration would normally be the greatest. The hydride film will coarsen and grow from the surface into the metal. This is shown schematically in Figs. 7a and 7b. As the hydride coarsens, hydrogen ingress becomes more and more difficult due to compression of the beta lattice. At some critical film thickness the hydride film will fracture brittly because it can no longer withstand the applied load (Fig. 7c) and the crack rapidly becomes arrested by plastic deformation as it enters the ductile substrate (Fig. 7d). Once the crack is arrested, the process is repeated, and hydrogen is again free to move preferentially in the beta lattice and form another titanium hydride film in the alpha-phase (Fig. 7e) which again undergoes brittle fracture (Fig. 7f). The discontinuous nature of this process will result in a fracture surface containing a terrace-like structure (Fig. 7g) and failure will be by cleavage in the brittle hydride located on the (1010) planes of alpha titanium at the alpha-beta boundaries. From this model, plastic tearing would be expected along the edges of each terrace step as the crack propagates from the brittle hydride into the ductile substrate. This is, of course, what is observed (see Fig. 6).

## Application of the Film-Rupture Model

Terrace steps width and hydrogen-induced crack growth rate are strongly influenced by the magnitude of applied stress intensity (Figs. 2 and 3), temperature (Fig. 3), and hydrogen pressure (Table I). According to the film-rupture model developed above for acicular titanium, the rate of hydrogen-induced crack growth is controlled by the rate of hydride film formation at the alpha-beta boundaries. It is assumed that failure of the hydride film occurs when the film grows laterally to a thickness which is no longer capable of carrying the applied load. The thicker the hydride film required before the rupture takes place, the deeper will be the hydride growth into the metal ahead of the crack tip, the longer will be the time required to attain this critical thickness [Eq. (7)], and the slower will be the observed rate of crack growth [Eq. (3)]. In the following sections, an attempt is made qualitatively to test this theory of hydrogen-induced crack growth with the experimental observations of this study for the purposes of evaluating the film-rupture model as applied to titanium and to understand better the overall process of hydrogen-induced crack growth.

### The Influence of Applied Stress Intensity

At low stress intensities, in the region of Stage I crack growth, an increase in stress intensity results in a rapid increase in crack growth rate (Fig. 3) and a decrease in terrace step width (Fig. 4). According to the film-rupture theory, this occurs because of a decrease in the critical thickness required for film rupture. An increase in stress intensity results in an increase in applied load at the tip of the crack. An increase in applied load across the brittle film will result in a decrease in the film thickness capable of withstanding this load. If this is the case, step width (i.e., film depth) will decrease because less time is available for film growth and thus, crack growth rate will increase — making theory and experiment in qualitative agreement.

Stage II (Fig. 3) is more difficult to explain in terms of the film-rupture theory. One explanation, which appears reasonable, is that at the transition between Stages I and II, the stress at the tip of the crack is equal to the yield stress of the material; thus, any increase in applied stress intensity only increases the size of the yield zone but does not increase the applied load across the brittle hydride film. The result, according to the film-rupture model, would be a constant critical thickness with increasing stress intensity in Stage II and a constant crack growth rate. The movement of the transition to higher stress intensities with decreasing temperature (Fig. 3) could be due in part to an

increase in the yield strength of the material requiring a greater applied stress intensity to reach yield at the crack tip.

### **The Influence of Temperature**

A decrease in temperature is seen to shift the crack growth rate-stress intensity curve to lower crack growth rates or higher stress intensities (Fig. 3). In terms of the film-rupture theory, temperature will have a direct influence on the rate of hydride film growth by lowering the hydrogen solid-solution solubility and decreasing the rate of hydrogen movement in the beta lattice. Therefore, under similar conditions of stress intensity and hydrogen pressure, a decrease in temperature will decrease the rate of film coarsening and preferential growth into the metal and it will take longer to obtain the critical film thickness for film rupture. The result will be to decrease the observed rate of hydrogen-induced crack growth and/or to increase the stress intensity required to obtain a given crack growth rate. The activation energy of approximately 10 Kcal/mole observed for Stage II growth (Fig. 3) is consistent with these ideas. The greater temperature dependence of Stage I (Fig. 3) may in part be due to the additional influence of the temperature dependence of the yield strength as discussed above.

### **The Influence of Hydrogen Pressure**

The influence of hydrogen pressure is similar to the influence of temperature in that a decrease in hydrogen pressure results in a decrease in hydrogen solid-solution solubility in the beta lattice. Again, such a decrease requires a greater time to obtain the required critical thickness for film rupture and thus, will decrease the observed hydrogen-induced crack growth rate at a given applied stress intensity (Table I).

### **SUMMARY**

The terrace-like fracture morphology associated with gaseous hydrogen-induced crack growth in acicular alpha-beta titanium alloys having an acicular microstructure was studied in detail. It was established that both hydrogen-induced crack growth rate and terrace step width varied with applied stress intensity, hydrogen pressure, and test temperature. An inverse exponential relationship was

found to exist between crack growth rate and step width. The relationship was independent of the variables of specimen configuration, magnitude of applied stress intensity, hydrogen pressure, and temperature within the resolution of this study. This inverse relationship was assumed to be due to the logarithmic growth of titanium hydride in the alpha-phase at the alpha-beta boundaries. The behavior was consistent with a model for hydride film growth in acicular titanium based on the time-dependent blocking of the beta-phase to preferential hydrogen transport. Next, the film-rupture model of stress corrosion cracking was applied to this model for hydride film growth. Finally, the film-rupture model, as modified for acicular titanium, was qualitatively applied to the data to explain the observed influences of stress intensity, test temperature, and hydrogen pressure.

## REFERENCES

1. H. G. Nelson, D. P. Williams, and J. E. Stein: *Met. Trans.*, 1972, vol. 3, pp. 469-75.
2. D. P. Williams and H. G. Nelson: *Met. Trans.*, 1972, vol. 3, pp. 2107-13.
3. D. A. Meyn: *Met. Trans.*, 1972, vol. 3, pp. 2302-5.
4. G. F. Pittinato and W. D. Hanna: *Met. Trans.*, 1972, vol. 3, pp. 2905-9.
5. M. J. Blackburn: *Trans. ASM*, 1966, vol. 59, pp. 876-89.
6. C. D. Beachem: Report of NRL Progress, Naval Research Laboratory, September 1969, pp. 36-7.
7. H. G. Nelson: *Met. Trans.*, 1973, vol. 4, pp. 364-66.
8. T. P. Papazoglou and M. T. Hepworth: *Trans. TMS-AIME*, 1968, vol. 242, pp. 682-85.
9. C. M. Craighead, G. A. Lenning, and R. I. Jaffee: *Trans. AIME*, 1956, vol. 206, pp. 923-28.
10. S. Mostovoy, P. B. Crosley, and E. I. Ripling: *J. Mater.*, 1967, vol. 2, pp. 661-81.
11. D. P. Williams and A. G. Evans: *J. Test. and Eval.*, 1973, vol. 1, pp. 264-70.
12. N. F. Mott: *Trans. Faraday Soc.*, 1939, vol. 35, p. 1175.
13. P. T. Lansberg: *J. Chem. Phys.*, 1955, vol. 23, p. 1079.
14. U. R. Evans: *The Corrosion and Oxidation of Metals*, Edward Arnold, London, 1960.
15. E. Davies, U. R. Evans, and J. N. Agar: *Proc. Roy. Soc. (London)*, 1954, vol. A225, pp. 443-62.
16. W. W. Mueller: *Metal Hydrides*, Academic Press (W. Mueller, J. Blakledge, and G. Libowitz, ed.), New York, pp. 386-440, 1968.
17. A. J. Forty: *Physical Metallurgy of Stress-Corrosion Fracture* (T. N. Rhodin, ed.), Interscience, New York, p. 99, 1959.
18. A. J. Forty and P. Humble: *Phil. Mag.*, 1963, vol. 8, p. 247.
19. A. J. McEvily, Jr. and A. P. Bond: *Electrochem. Soc.*, 1965, vol. 112, p. 131.
20. E. N. Pugh: *The Theory of Stress Corrosion Cracking in Alloys* (J. C. Scully, ed.), NATO, Brussels, pp. 418-41, 1971.

**Table I. Variation in Crack Growth Rate and Step Width as a Function of Hydrogen Pressure for Ti-6Al-4V-DT Specimens at a Constant Stress Intensity in Stage II ( $76 \text{ MN m}^{-3/2}$ ) at  $24^\circ \text{C}$**

Hydrogen Pressure $P_{\text{H}_2}, \text{ kN m}^{-2}$	Crack Growth Rate $da/dt, \text{ m s}^{-1}$	Step Width $X, \text{ m}$
90.6	$1 \times 10^{-4}$	3.25
90.6	$9 \times 10^{-5}$	3.5
75	$8 \times 10^{-5}$	3.5
60.8	$3.6 \times 10^{-5}$	4.25
48.8	$4.75 \times 10^{-5}$	4.25
6.1	$7.2 \times 10^{-6}$	5.25





40  $\mu\text{m}$

Fig. 1 SEM of the fracture surface of Ti-6Al-4V alloy having an acicular microstructure and failed in gaseous hydrogen at a pressure of  $90.6 \text{ kN m}^{-2}$  (680 torr). Arrows indicate the probable direction of local crack growth.

**PRECEDING PAGE BLANK NOT FILMED**

ORIGINAL PAGE IS  
OF POOR QUALITY

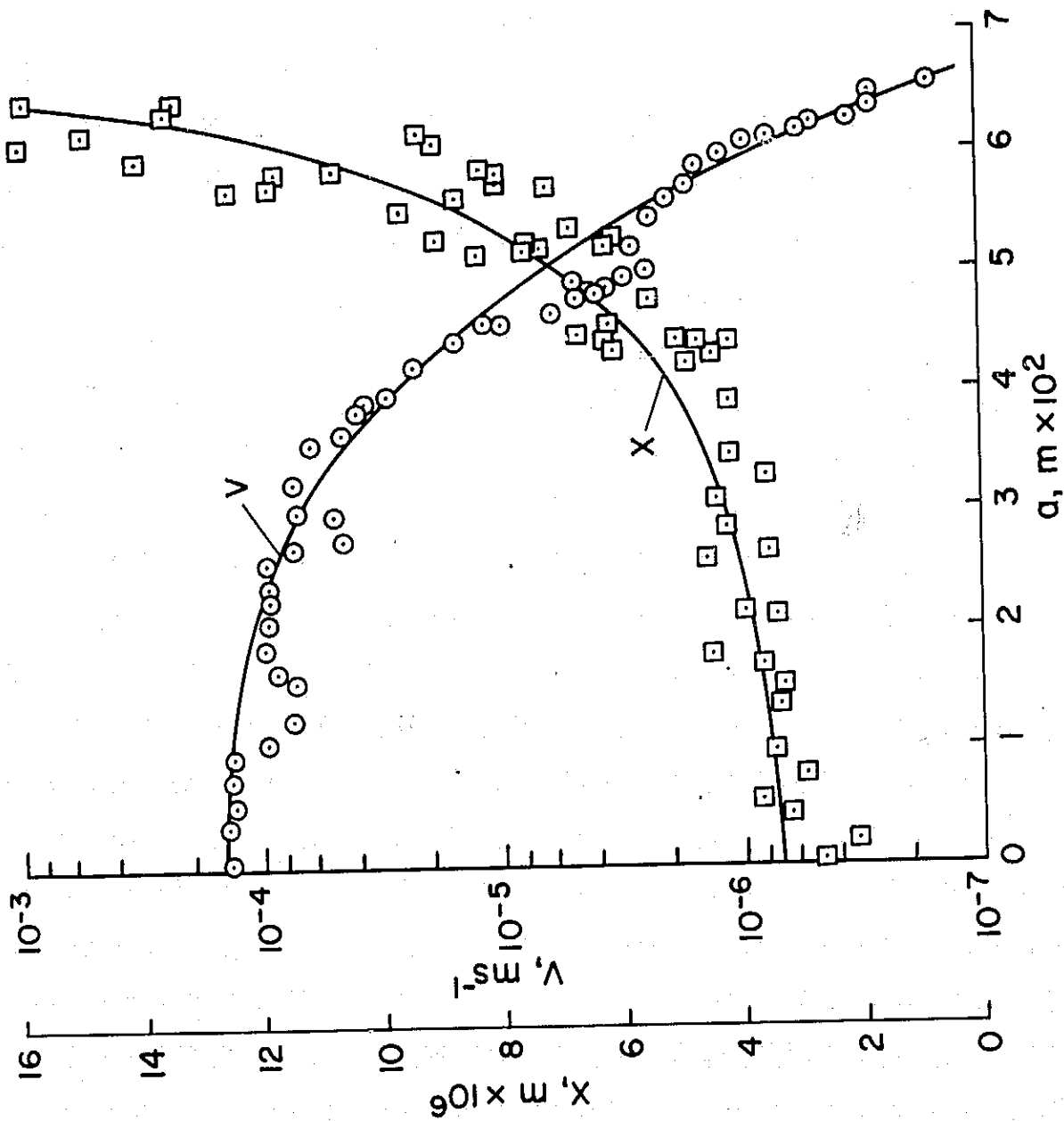


Fig. 2—Variation in terrace step width and hydrogen-induced crack growth rate as a function of crack length in a Ti-6Al-4V DT specimen tested in gaseous hydrogen ( $P = 90.6 \text{ kN m}^{-2}$ ,  $T = 24^\circ\text{C}$ ).

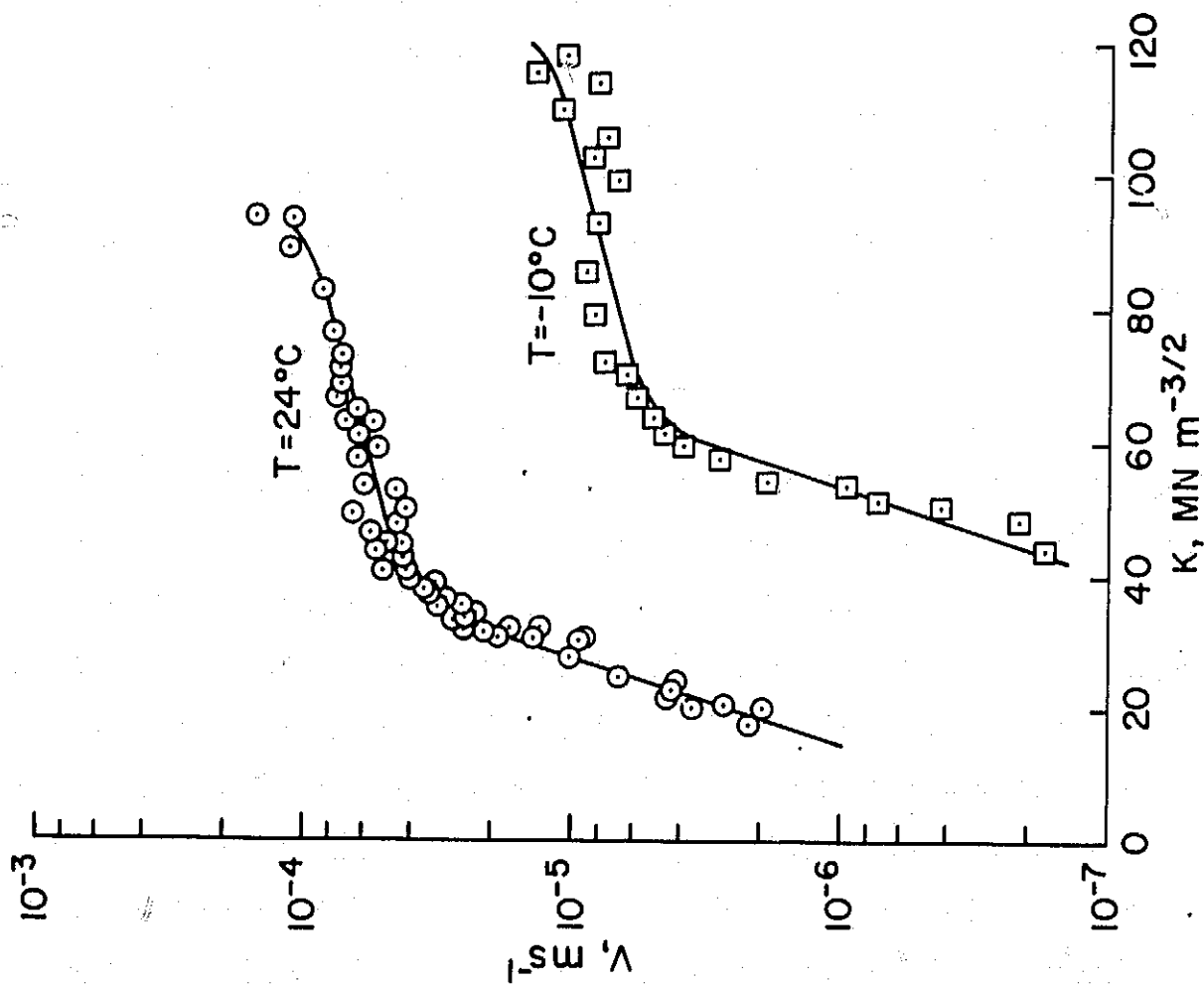


Fig. 3—Hydrogen-induced crack growth as a function of applied stress intensity for Ti-6Al-4V DCB specimens tested at  $24^\circ\text{C}$  and  $-10^\circ\text{C}$  ( $P = 90.6 \text{ kN m}^{-2}$ ).

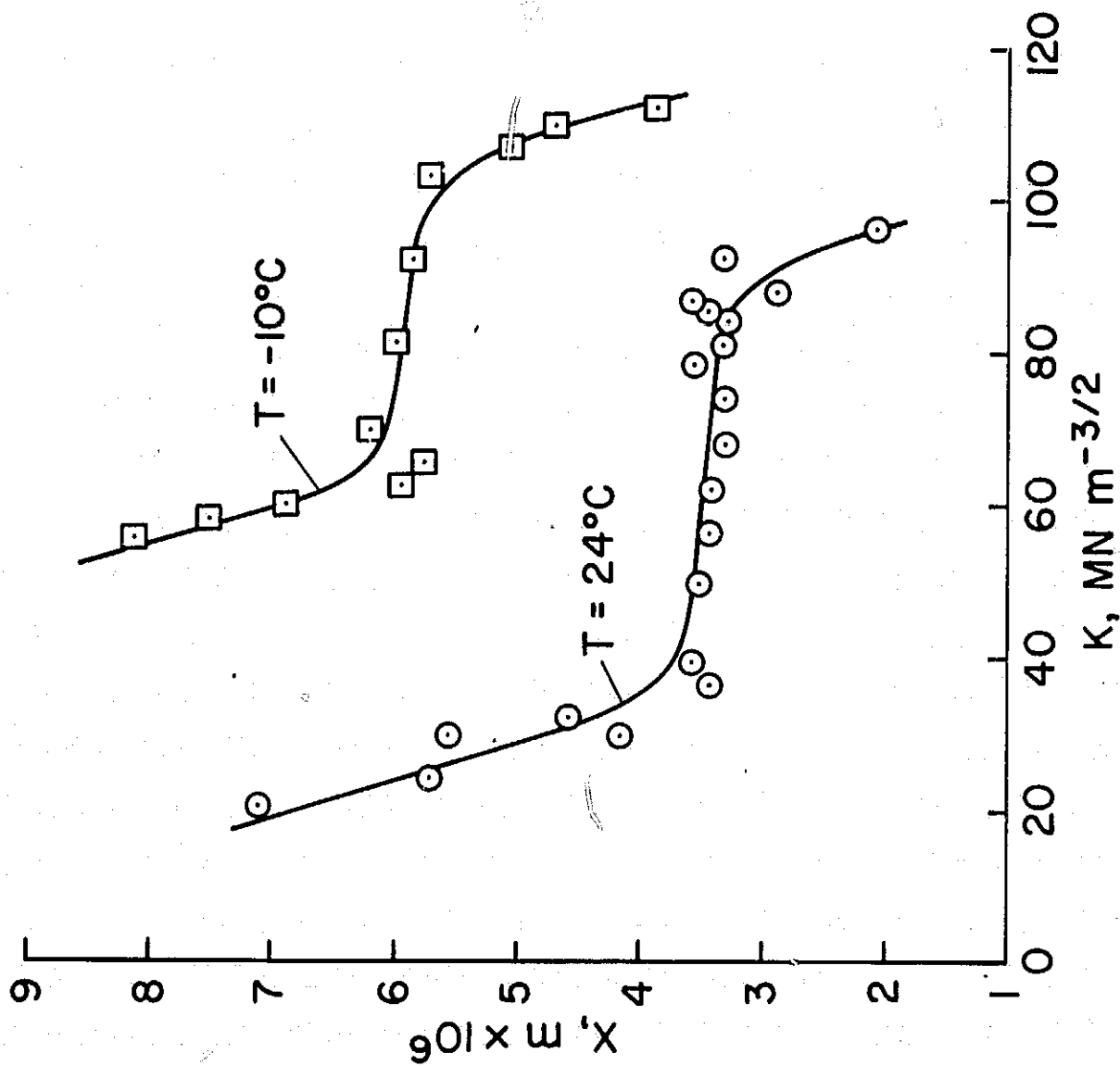


Fig. 4—Variation in step width as a function of applied stress intensity for Ti-6Al-4V DCB specimens tested at  $24^\circ\text{C}$  and  $-10^\circ\text{C}$  ( $P = 90.6 \text{ kN m}^{-2}$ ).

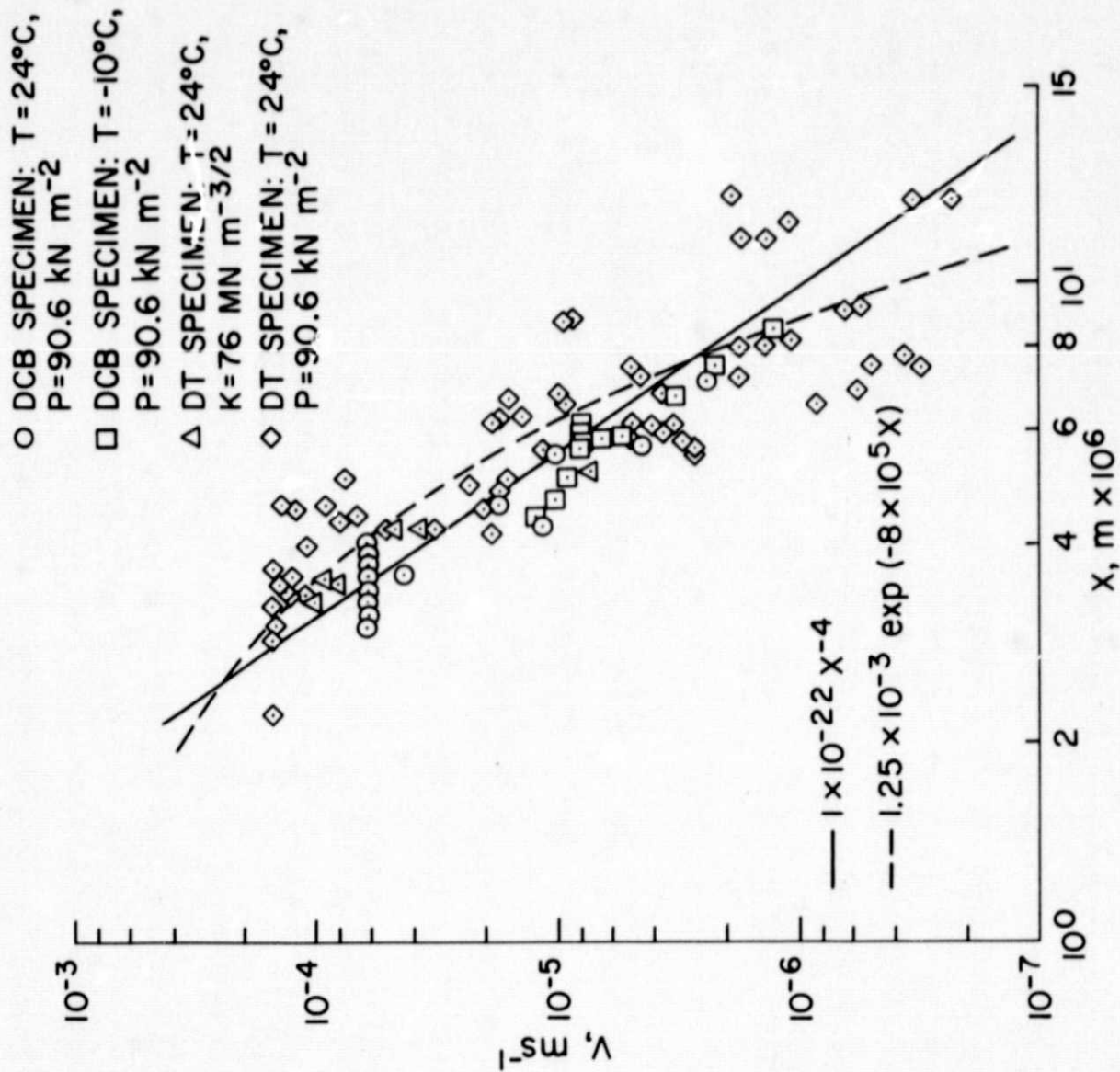


Fig. 5—Hydrogen-induced crack growth as a function of average step width observed on the fracture surfaces of DT and DCB specimens tested at various stress intensities, temperatures, and hydrogen pressures.

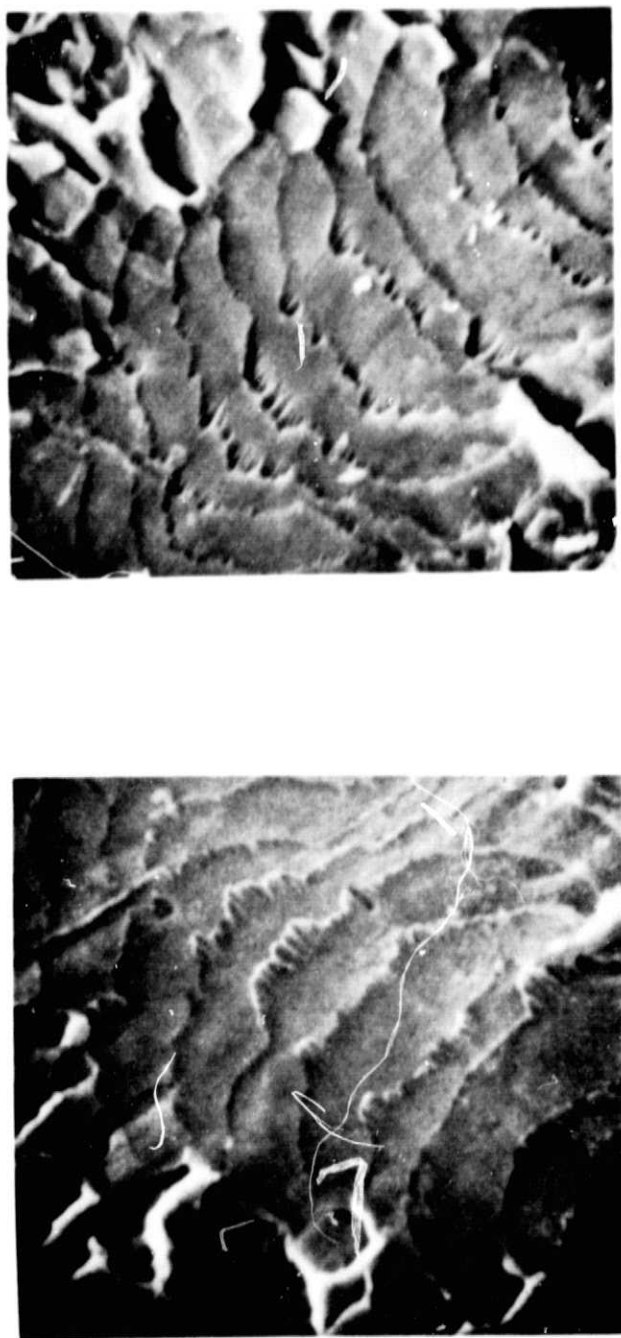


Fig. 6—Mating fracture surfaces showing considerable plastic deformation associated with the terrace steps.

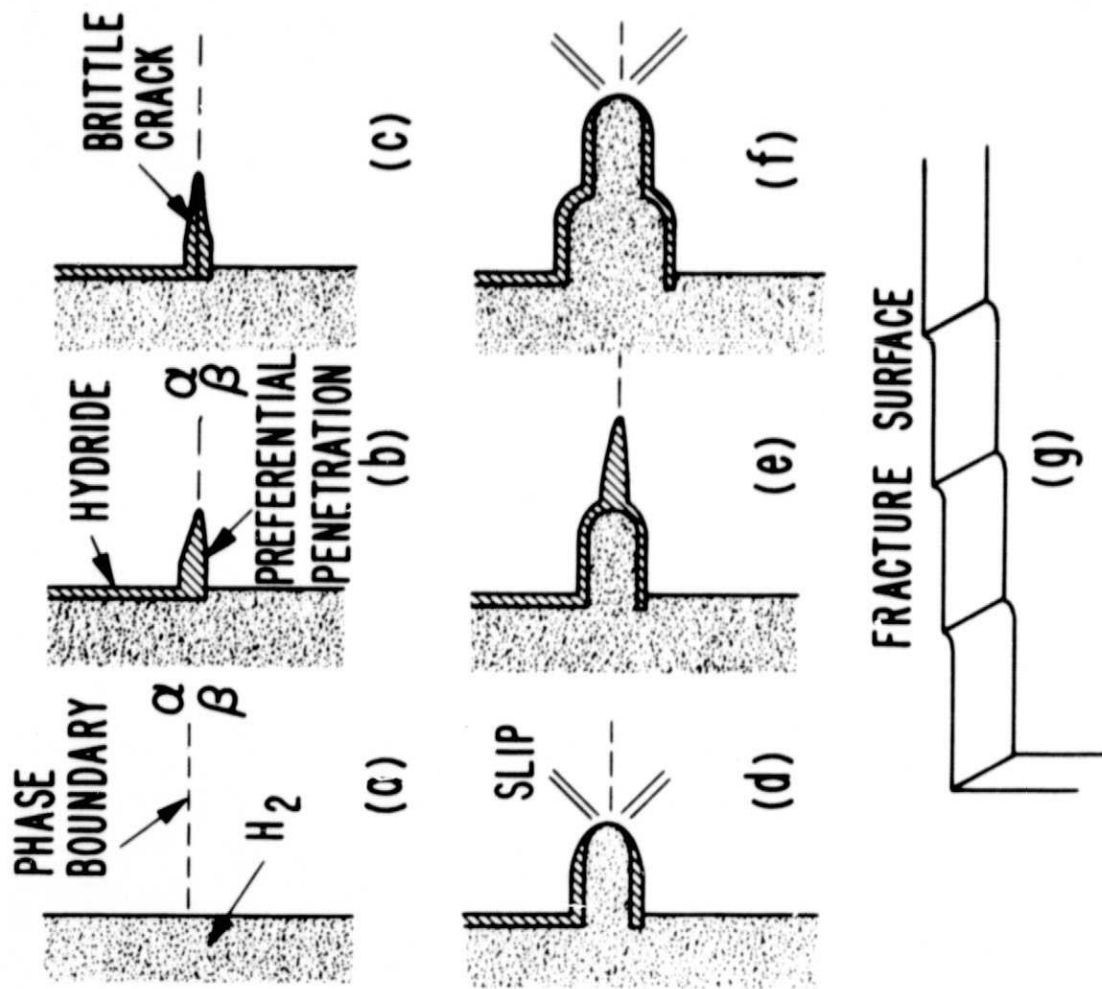


Fig. 7—The film-rupture theory of stress corrosion cracking applied to the model of hydrogen-induced cracking of titanium.